ADSORPTION OF ZINC AND COPPER IONS ON NATURAL AND ETHYLENEDIAMINE MODIFIED MONTMORILLONITE

ONDŘEJ KOZÁK, PETR PRAUS, VLADIMÍR MACHOVIČ*, ZDENĚK KLIKA

Department of Analytical Chemistry and Material Testing, VŠB-Technical University of Ostrava, 17. listopadu 15, 708 33 Ostrava-Poruba, Czech Republic
**Central Laboratory, Institute of Chemical Technology Prague, Technická 5, 166 28 Prague, Czech Republic*

E-mail: petr.praus@vsb.cz

Submitted April 16, 2009; accepted December 18, 2009

Keywords: Adsorption, Intercalation, Zinc, Copper, Montmorillonite, Ethylenediamine

In this study, adsorption of the zinc and copper ions on montmorillonite (MMT) was investigated. In all experiments performed at pH 6.4 to 4.8, the Langmuir-Freundlich isotherm was found to best fit adsorption data that confirms a monolayer formation of the metals. The maximum amounts of the adsorbed metals did not exceed a cation exchange capacity (CEC) of MMT. UV-VIS diffuse reflectance spectrometry reveals no complexes between Zn^{2+} or Cu^{2+} and MMT and thus the metal uptake took part only by ion exchange. X-ray diffraction (XRD) patterns indicated an intercalation of the metal ions into the montmorillonite interlayer. In addition, using thermogravimetry and infrared spectrometry it was found the intercalated metals create aqua complexes $[Zn(H_2O)_6]^{2+}$ and $[Cu(H_2O)_6]^{2+}$. In order to increase the adsorbed amounts of Zn^{2+} and Cu^{2+}, MMT was previously intercalated with ethylenediamine (EDA-MMT). EDA caused an increase of the adsorbed copper ions about 28 % due to the formation $[Cu(EDA)_2]^{2+}$ in the interlayer as was confirmed by the infrared spectrometry. Adsorbed amounts of the zinc ions on EDA-MMT was 3-4 folds higher than CEC but no complex with EDA was observed. This effect was explained by expansion of a space between the montmorillonite layers, which facilitates the intercalation of the zinc ions and nitrate compensating the excessive positive charge.

INTRODUCTION

Phyllosilicates are layered silicates, in which the SiO_4 tetrahedra are linked together in infinite two-dimensional sheets and are condensed with the layers of AlO_6 or MgO octahedra in the ratio 2:1 or 1:1. The negatively charged layers attract positive cations (Na^+, K^+, Ca^{2+}, Mg^{2+}) that can hold the layers together. Their high cation exchange capacities enable them to adsorb heavy metals and quaternary salts [1,2] including cationic surfactants [3].

Through laboratory as well as field experiments, the adsorption of heavy metals on phyllosilicates has been studied. Most often smectites or smectitic soils and sediments have been the objects of this research because of their high CECs and specific surface areas. The adsorption of heavy metals M^{2+} (Cd, Pb, Cu, Mn, Zn and Co) on clay minerals, metal hydroxides, and organic matter, has been described by empirical and mechanistic models [4-7]. Phyllosilicates were evaluated to be used as remedial agents in contaminated waste deposits [8].
Generally, a model of cation adsorption on clay minerals implies (i) a pH-independent adsorption through cation exchange reactions on permanent negative sites and (ii) a pH-dependent surface complexation on surface silanol (≡SiOH) and aluminol (≡AlOH) sites [9-11]. The complexation mechanism with the edge-surface silanol and aluminol groups [7,9,10] creates inner-sphere monodentate or bidentate complexes. For example, a formation of the inner sphere complex of Zn^{2+} and montmorillonite was suggested by Ikhsan et al. [12]. Another way of the metal adsorption is its complexation to MMT by the creation of so-called outer-sphere complexes [7].

Many studies deal with the montmorillonite intercalation by the metal cations [10,13,14]. There are also some studies carried out to examine the adsorption of heavy metals on montmorillonite modified with various organic cations [15], pyridine [16], alkylammonium cationic surfactants and polymeric Fe- and Al-polyoxocations $[Al_{13}O_4(OH)_{24}(H_2O)_{12}]$ [5]. These modifications cause changes of the MMT adsorption capacity.

The aim of this work was to study the adsorption of environmentally important heavy metals, such as zinc and copper, on montmorillonite, which is a typical representative of phyllosilicates. Phyllosilicates could be suitable adsorbents for the retention of toxic metals occurring in polluted water and soils.

EXPERIMENTAL

Material and chemicals

Reagents

The used chemicals were of analytical reagent grade: zinc nitrate, copper sulphate, ammonium chloride, ethylenediamine (all from Lachema, Czech Republic). Water deionised by reverse osmosis (Aqua Osmotic, Czech Republic) was used for the preparation of all solutions.

Na^+-rich montmorillonite Wyoming (SWy 2) (Crook County, Wyoming) with CEC of 1.21 ± 0.06 meq g^{-1} determined by the saturation with NH_4^+ [17] was used for all adsorption experiments. The structural MMT formula is $Na_{0.38}K_{0.04}(Ca_{0.12}\ Mg_{0.50}\ Fe^{3+}_{0.41}\ Al_{2.90}\ Ti_{0.01}\ Mn_{0.01})(Si_8)\ O_{20}(OH)_4$ as calculated from the results of X-ray fluorescence analysis. A fraction of MMT with particle size < 5 μm separated by sedimentation was used.

Adsorption procedure

EDA-MMT was prepared by shaking MMT in conc. ethylenediamine (0.9 g/cm^3) for 24 hours, filtering and drying at 105°C for 2 hours. MMT and EDA-MMT were fully saturated by the metals by their shaking in the solutions of 5 mmol/l of Cu^{2+} and 20 mmol/l of Zn^{2+}, respectively, at 170 rpm for 24 hours. Then, the suspensions were centrifuged for 20 minutes, filtered and dried at 105°C for 2 hours. 0.85 μm filters (Pragochema, Czech Republic) were used for the filtration. The room temperatures varied from 20°C to 24°C during all experiments. The pH values of the solutions and suspensions were measured by a pH-meter inoLab (WTW, Germany).

MMTs saturated with Cu^{2+} and Zn^{2+} were denoted as Cu-MMT and Zn-MMT, respectively. Also another Zn-MMT intercalate at the concentration of 0.5 mmol l^{-1} (Zn0.5-MMT) was prepared for the purpose of infrared study.

The filtrates were analysed for zinc and copper using atomic absorption spectrometry (AAS) [18]. Contents of the copper ions adsorbed on montmorillonite were determined by AAS after a dissolution of the MMT samples in a mixture of HF, HNO_3 and $HClO_4$ (5:4:4) [19].

Methods

Atomic absorption spectrometry

Concentrations of the metal ions before and after adsorption and in the dissolved montmorillonite samples were measured by atomic adsorption spectrometer AA280FS (Varian Inc., Austria) with the acetylene-air atomization. The measured data were processed by the SpectrAA Pro software.

X-ray powder diffraction

X-ray powder diffraction study was performed by a powder diffractometer (INEL, France) equipped with a curved position-sensitive detector PSD 120 MB/11 (reflection mode, Ge-monochromatized, CuKα1 radiation). Diffraction patterns were taken in ambient atmosphere under constant conditions (1500 s, 60 kV, 55 mA).

Fourier transform infrared spectrometry

Infrared (IR) spectra were obtained by the KBr method using a Nicolet NEXUS 470 Fourier transform (FTIR) spectrometer (Thermo Nicolet Instrument Co., Madison, USA). The spectrometer was equipped with a Globar IR source, KBr beam splitter, and DTGS detector. For each spectrum, 128 scans were obtained with the resolution of 4 cm^{-1}. The obtained IR spectra were processed by means of the program OMNIC 7.3.

Another infrared spectra were measured by the diffuse reflectance technique (DRIFT) using a Nicolet 7600 spectrometer (Thermo Nicolet Instrument Co., Madison, USA). The technical specifications were the same as in case of the spectrometer used for the KBr method.

Diffuse reflectance UV-VIS spectrometry

UV-VIS Diffuse reflectance spectra (DRS) were obtained using a Perkin Elmer Lambda 35 spectrometer equipped with an integrating sphere (Labsphere). The spectra of these powders were measured in circular cells with quartz windows between 250 nm and 1100 nm (40000-9090 cm^{-1}) with a 0.5 nm step.

Thermal analysis

Thermal analysis was performed by means of thermogravimetry (TG) and differential thermal analysis (DTA). The TG and DTA curves were obtained using an instrument Netzsch, STA 409. The measurements were performed in ceramic crucibles under static air atmosphere at the heating rate of 10°C/min and 5°C/min. Approximately 100 mg of natural and intercalated montmorillonites were used for each measurement.

Adsorption isotherms

Analysis of equilibrium concentrations

The adsorption isotherms of Cu^{2+} and Zn^{2+} were determined by means of batch experiments. Experimental data were fitted with several common adsorption isotherms: Langmuir, Freundlich, generalised Langmuir-Freundlich (also called Sips isotherm [20,21]), Temkin and Dubinin-Radushkevich isotherms. A non-linear regression was performed by the Gauss-Newton iteration method (QC.Expert 2.5, Trilobyte, Pardubice). The best fitting regression model was chosen according to statistical criteria: regression coefficient (R), the Akaike information criterion (AIC) and the mean error of prediction (MEP).

RESULTS AND DISCUSSION

Adsorption of Zn^{2+} and Cu^{2+} on MMT

The adsorption experiments were evaluated by the adsorption isotherms mentioned above. The equilibrium concentrations of Zn^{2+} and Cu^{2+} [22] were determined by AAS. The metal amounts adsorbed on MMT a (meq/g) were calculated as follows:

$$a = \frac{(c_0 - c_e)V}{w} \quad (1)$$

where c_0 and c_e are the initial and equilibrium concentrations (mmol/l), respectively V (l) is a volume of the metal salts solutions and w (g) is a mass of MMT.

Using the non-linear regression, the appropriate adsorption isotherm was chosen for each experiment according to the statistical criteria R, AIC and MEP. The regression results are summarised in Table 1. In case of the Zn^{2+} adsorption, the best fitting isotherm was the Langmuir-Freundlich one (Figure 1)

$$a = a_m \frac{(bc_e)^p}{1+(bc_e)^p} \quad (2)$$

where a (mmol/g) and c_e (mmol/l) are the adsorbed amount of the metals on MMT and their equilibrium concentration, respectively, and p is a power constant. As this equation has three fitting constants, it much better describes the adsorption including binding interactions among adsorbing compounds [21]. The found constants are a_m = 1.08 ±0.07 (meq/g), b = 5.27 ± 1.41 (l/mmol), p = 0.70 ± 0.13 for Zn^{2+} (n = 15) and a_m = 0.76 ± 0.06 (meq/g), b = 0.76 ± 0.06 (l/mmol), p = 0.75 ± 0.45 for Cu^{2+} (n = 10). The exponent p was always lower than 1, which indicates the negative adsorption co-operativity as a result of the repulsive electrostatic forces between the metal ions. The regression results also indicate both the adsorbed Zn^{2+} and Cu^{2+} ions were arranged in their monolayers. The maximum adsorbed amounts were lower than CEC in both cases.

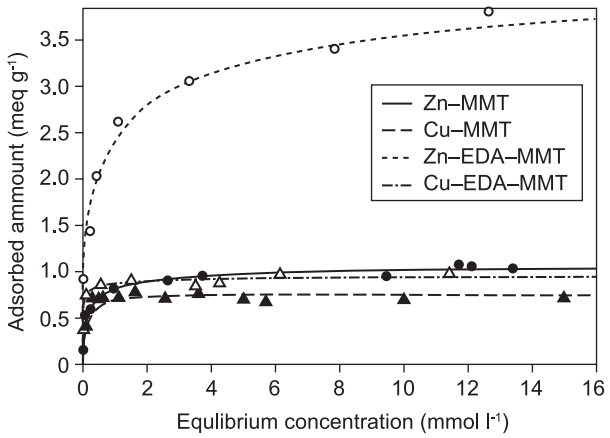

Figure 1. Langmuir-Freundlich adsorption isotherms of Zn^{2+} and Cu^{2+}.

Table 1. Isotherm parameters of Zn^{2+} and Cu^{2+} adsorption on MMT.

	Adsorption isotherm		
Zinc ions	R	AIC	MEP
Langmuir	0.989	-87.4	0.00305
Freundlich	0.945	-67.6	0.01110
Langmuir-Freundlich	0.994	-98.7	0.00143
Temkin	0.981	-83.4	0.00402
D-R	0.973	-78.4	0.00529
Copper ions			
Langmuir	0.961	-63.9	0.003
Freundlich	0.838	-50.4	0.009
Langmuir-Freundlich	0.969	-64.1	0.004
Temkin	0.874	-52.7	0.007
Dubinin-Radushkevich	0.972	-67.1	0.001

At the Cu^{2+} equilibrium concentrations above 5 mmol l^{-1}, the Equation (1) could not be used because the Cu^{2+} ions were also highly adsorbed on the surface of PE reaction vessels. Therefore, the adsorbed amounts were found by the analysis of dissolved Cu-MMT in a mixture of mineral acids (see Material and Chemicals).

The adsorption mechanisms of the metal adsorptions were studied by the measurements of UV-VIS DRS of Zn-MMT and Cu-MMT. Only in case of Cu-MMT, these spectra showed one absorption band at about 720 nm, which corresponds to the adsorption of the free Cu^{2+} ions. It corresponds with the bright blue colour of Cu-MMT. No other absorption bands corresponding to the charge transfer O→Zn^{2+} and O→Cu^{2+} documenting the MMT surface complexation referred by Ding and Frost [23] were observed. Therefore, both Zn^{2+} and Cu^{2+} should be adsorbed only due to their ion exchange reactions with the interlayer cations, mostly Na^+. It well corresponds with the pH dependent speciation of Cu^{2+} in the MMT system calculated by Stadler and Schindler [24]. A percentage of the exchanged metals was 89.3 % for Zn^{2+} and 62.8 % for Cu^{2+} of CEC.

During the adsorption study, pH of the metal solutions was also measured. As zinc nitrate as well as copper sulphate are salts of strong acids and weak bases, the pH values of their solutions were weakly acid, from 5.5 to 4.5. The adsorption experiments started at these pH values. The pH values of the equilibrium solutions of Cu^{2+} and Zn^{2+} varied from 6.0 to 4.8 and from 6.4 to 5.8, respectively, with the increasing concentrations of both metals. It is obvious that pH in these solutions increased after the adsorption, which is caused by the ion exchange of the interlayer cations with the hydrogen ions.

Adsorption of Zn^{2+} and Cu^{2+} on EDA-MMT

In order to increase the adsorbed amounts of the metals, montmorillonite was modified by EDA prior to the adsorption experiments. EDA is known as a reagent

forming complexes with many metals, specially with Cu^{2+} as $[Cu(EDA)_2]^{2+}$. This complex is stable and not altered in aqueous solutions and is also strongly stabilized in montmorillonite by the ion exchange at low pH [24]. Due to these properties, $[Cu(EDA)_2]^{2+}$ has been used for the determination of CEC of phyllosilicates [25].

The metal adsorptions on EDA-MMT were examined in the same manner as on natural MMT. The obtained data were fitted with the already mentioned adsorption isotherms and the regression results are summarised in Table 2. The regression constants were estimated: $a_m = 4.70 \pm 1.56$ (meq g^{-1}), $b = 1.16 \pm 2.11$ (l/mmol), $p = 0.46 \pm 0.23$ ($n = 8$) for Zn^{2+} and $a_m = 0.97 \pm 0.17$ (meq/g), $b = 129 \pm 175$ (l/mmol), $p = 0.47 \pm 0.35$ for Cu^{2+} ($n = 7$). It is obvious the zinc ions were adsorbed on EDA-MMT in approximately 3-4 fold amounts than on MMT. The maximum adsorbed amount of Cu^{2+} increased about 28 %, that is, 80.1 % of CEC. It agrees with our idea of forming the stable copper complexes with EDA in the MMT interlayer.

Table 2. Isotherm parameters of Zn^{2+} and Cu^{2+} adsorption on EDA-MMT.

	Adsorption isotherm		
Zinc ions	R	AIC	MEP
Langmuir	0.967	-19.9	0.1168
Freundlich	0.975	-22.3	0.1143
Langmuir-Freundlich	0.990	-29.1	0.0620
Temkin	0.982	-25.8	0.0927
D-R	0.941	-14.1	0.2019
Copper ions			
Langmuir	0.949	0.115	-35.6
Freundlich	0.927	0.014	-33.2
Langmuir-Freundlich	0.981	0.003	-40.5
Temkin	0.955	0.012	-36.5
Dubinin-Radushkevich	0.975	0.005	-40.6

XRD study

XRD patterns were obtained to identify the intercalation of Cu^{2+}, Zn^{2+} into MMT and EDA-MMT (Figure 2). The measured interlayer spacings d_{001} are summarised in Table 3. The d_{001} value of Cu-MMT well agrees with the values of 1.23 and 1.25 nm found by Ding and Frost [23] and Németh et al. [14], respectively. In the XRD patterns no other crystalline structures, such as the zinc or copper hydroxides and oxides, were observed.

Table 3. Interlayer distances of MMT samples.

Material	d_{001} (nm)
MMT	1.22
EDA-MMT	1.30
Zn-MMT	1.34
Zn-EDA-MMT	1.25
Cu-MMT	1.24
Cu-EDA-MMT	1.23

It was recognised by electron spin echo modulation measured at 77 K and XRD [26] that the d_{001} values depend on the hydratation of Cu^{2+} in this way: $d_{001} = 2.0$ nm for $[Cu(H_2O)_6]^{2+}$, $d_{001} = 1.5$ nm for $[Cu(H_2O)_4]^{2+}$ and $d_{001} = 1.0$ nm for $[Cu(H_2O)]^{2+}$. The latter work of Morton et al. [27] based on X-ray absorption spectra suggested that Cu^{2+} intercalated in Ca-MMT (Cheto) are surrounded with four waters forming the outer-sphere complexes. In an electron paramagnetic resonance study of Hyun et al. [28] it was shown the copper ions exist in the MMT interlayer as the complex $[Cu(H_2O)_6]^{2+}$. He et al. [29] referred in their work that the presence of the hexaaqua-copper ions in the MMT interlayer was indicated by $d_{001} = 1.523$, which is contrary to the findings of Kevan [26] as mentioned above. It is clear that the literature results are not unambiguous and therefore it is hard to decide, which type of the aqua-Cu^{2+} complex exists between the MMT layers only on the basis of the d_{001} values. A molecular modelling of the Zn^{2+} intercalation in montmorillonite was performed by Janeba et al. [30] and $[Zn(H_2O)_6]^{2+}$ was found as the likeliest zinc specie. It should be completed that Zn^{2+} and Cu^{2+} are coordinated with the water molecules in aqueous solutions forming $[Zn(H_2O)_6]^{2+}$ and $[Cu(H_2O)_6]^{2+}$ complexes, respectively [31].

The MMT d_{001} value increased by the adsorption of EDA. The XRD pattern of EDA-MMT is shown in Figure 2. EDA is a weak base ($pK_{a,1} = 10$, $pK_{a,2} = 6.8$) and exists

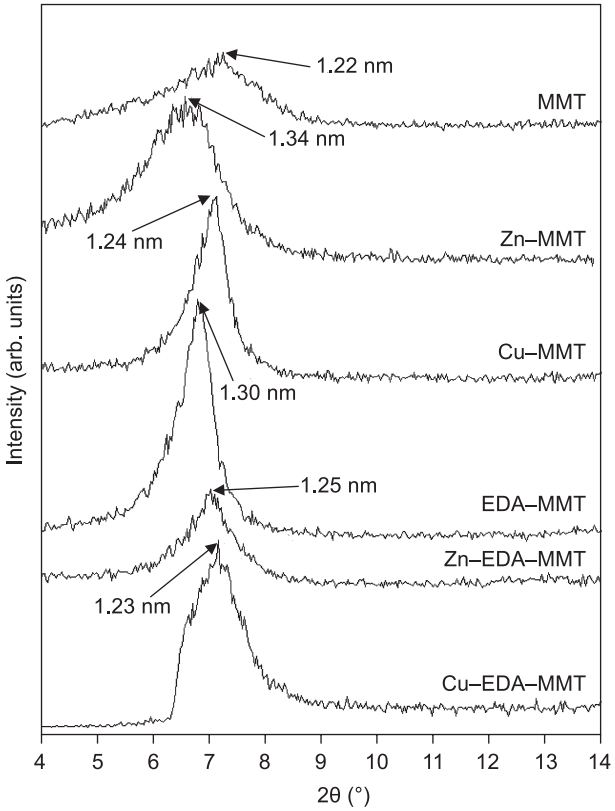

Figure 2. XRD patterns of MMT, Zn-MMT, Cu-MMT, EDA-MMT, Zn-EDA-MMT and Cu-EDA-MMT with the d_{001} values.

in the pH range used in our experiments as a divalent cation EDA^{2+}. Therefore, we suppose the intercalation of EDA^{2+} via the ion exchange reactions with the interlayer (sodium) ions. The presence of EDA in MMT was observed also in the infrared spectra (see below). We suppose that EDA forms the stable MMT intercalates because it was not removed from the interlayer during the preparation steps, such as washing and drying (see Material and Chemicals).

The adsorption of Zn^{2+} and Cu^{2+} on EDA-MMT was accompanied by a slight decrease of the d_{001} basal spacings. This effect should be explained by the re-ion exchange of EDA^{2+} with the metals and/or by different orientations of their EDA complexes between the MMT layers. In order to understand the role of EDA, the infrared spectra of MMT, Zn-MMT, Cu-MMT, Zn-EDA-MMT and Cu-EDA-MMT were obtained.

Infrared study

Infrared study by using the KBr method

The infrared spectra of the montmorillonite samples were obtained by the KBr method using an FTIR spectrometer. These spectra are demonstrated in Figures 3a and 3b. Figure 3a shows changes in the bands related to the stretching vibrations of $-NH_2$ (Area A) and $-CH_2-$ (Area B) groups and Figure 3b demonstrates the bending vibrations of the $-NH_2$ group (Area C).

In case of Zn^{2+}, absorbances of the stretching and bending vibrations decreased with the increasing content of Zn^{2+} in EDA-MMT until they completely disappeared. It can be explained by the release of EDA^{2+} from the interlayer due to the ion exchange with Zn^{2+} that does not react with EDA^{2+}. In addition, a sharp peak at about 1380 cm^{-1} in Figure 3b proves the presence of nitrate in Zn-EDA-MMT.

On the contrary, the stretching and bending vibration bands of Cu-EDA-MMT are still visible independently on the intercalated Cu^{2+} amounts. Therefore, the only one spectrum was shown in Figures 3a and 3b. In addition, a new band near 3300 cm^{-1} appeared (Figure 3a). It can be attributed to the stretching vibrations of the NH group indicating that EDA is still fixed in the montmorillonite interlayer forming the complex $[Cu(EDA)_2]^{2+}$.

Comparing these results with the XRD observations we can suppose that d_{001} of Cu-EDA-MMT decreased as a result of the $[Cu(EDA)_2]^{2+}$ orientation in the interlayer. In case of Zn-EDA-MMT, we can suppose that (i) EDA firstly expanded the interlayer space facilitating the intercalation of Zn^{2+} and NO_3^- compensating the excessive positive charge and (ii) then EDA was released by the re-ion exchange with Zn^{2+}.

Infrared study by using the DRIFT method

The DRIFT spectra are shown in Figure 4. These spectra were measured without a mixing with KBr to avoid the ion exchange reactions with the intercalated cations. A very strong band at 3636 cm^{-1} was attributed to the hydroxylic groups of AlAlOH in the MMT octahedra. Vibrations of the adsorbed water molecules bonded mutually by the hydrogen bonds are identified by a band at 3420 cm^{-1}. Kloproge et al. [32] used the band at 3630 cm^{-1} as an inner standard for estimation of the water content in MMT intercalated with Cu^{2+}. In this work, the water amount was characterised by a ratio of the absorbances measured at 3420 cm^{-1} and 3636 cm^{-1}.

A column diagram in Figure 5 demonstrates the amounts of interlayer water related to the interlacated cations. As obvious, Cu-MMT contains the similar amount of interlayer water as Zn-MMT. It indicates that both metals should create the aqua-complexes with the same number of water molecules.

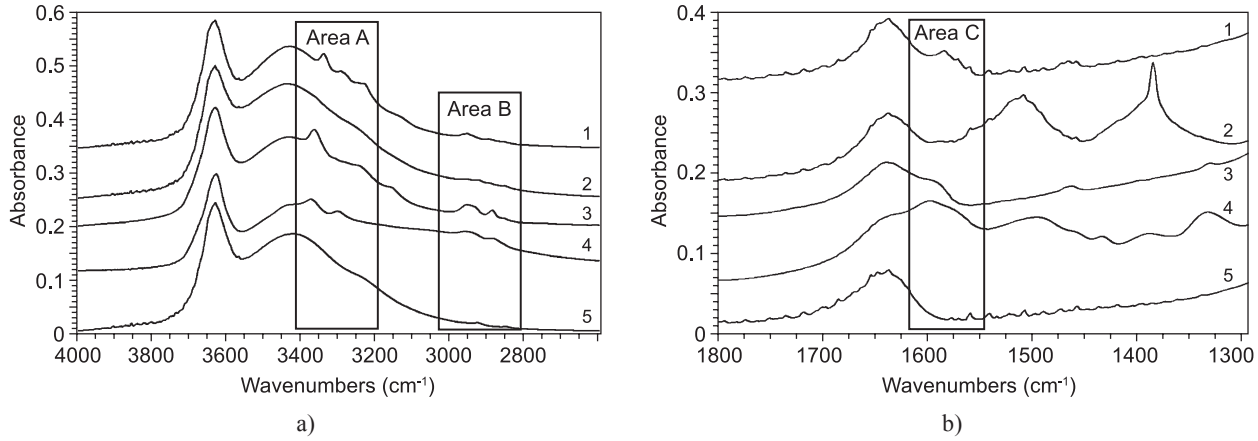

Figure 3. Infrared spectra of MMT (5), EDA-MMT (4), Zn-EDA-MMT saturated at 0.5 mmol l^{-1} (3) and 20 mmol l^{-1} (2) of Zn^{2+} and Cu-EDA-MMT saturated at 5 mmol l^{-1} of Cu^{2+} (1) - a) within 3900 cm^{-1} to 2700 cm^{-1}, b) within 1900 cm^{-1} to 1300 cm^{-1}.

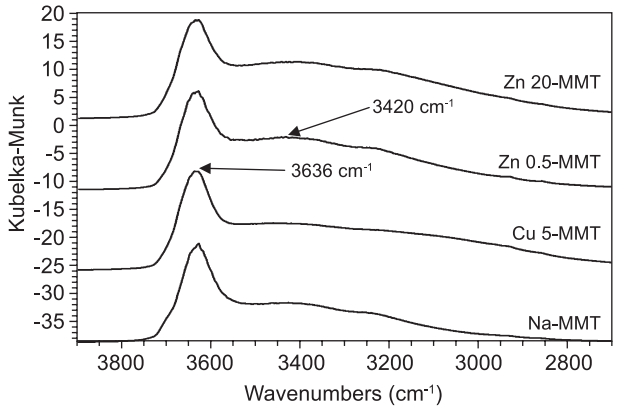

Figure 4. DRIFT spectra of MMT, Cu-MMT and Zn-MMT.

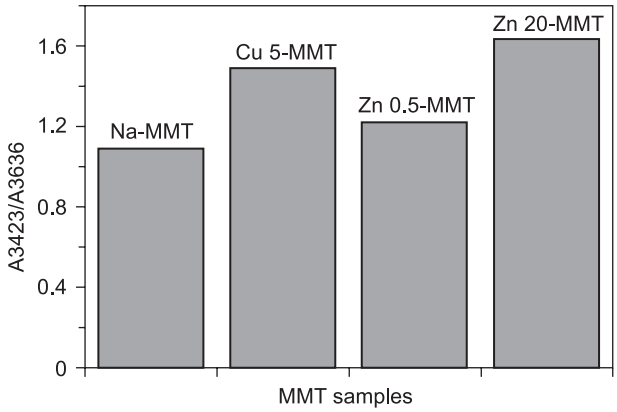

Figure 5. Content of water in the MMT interlayers expressed via a ration of absorbances at 3423 cm^{-1} and 3636 cm^{-1}.

Thermal analysis

An another attempt to find out the amount of water complexing the metal ions in the MMT interlayer was performed by the thermal analysis of MMT, Cu-MMT and Zn-MMT. In general, during heating montmorillonite loses its mass in three steps: (i) desorption of water adsorbed on MMT, (ii) dehydration of the hydrated interlayer cations and (iii) dehydroxylation of the MMT structure [33]. Figure 6a shows the TG and DTA curves of MMT in the range from 25°C to 1000°C at the heating rate of 10°C/min. Figures 6b shows the curves of MMT, Zn-MMT and Cu-MMT measured in the narrower temperature interval from 25°C to 475°C at the heating rate of 5°C/min.

From the TG curves (Figure 6b), the loss of interlayer water of MMT, Zn-MMT and Cu-MMT was calculated. As the a_m values were lower than CEC, amounts of the interlayer water n_w co-ordinating Zn^{2+} or Cu^{2+} were calculated as a difference between the amounts of total interlayer water $n_w(M\text{-}MMT)$ and free interlayer water $n_{w,free}(M\text{-}MMT)$ (non-complexing the metals) in the MMT intercalate

$$n_w = n_w(M\text{-}MMT) - n_{w,free}(M\text{-}MMT) \qquad (3)$$

The $n_w(M\text{-}MMT)$ values were calculated as the water amount released during the dehydration of Zn-MMT and Cu-MMT. Free water in the Zn-MMT and Cu-MMT interlayer was estimated using the amount of interlayer water in natural MMT $n_w(MMT)$ and CEC as follows

$$n_{w,free} = n_w(MMT)\frac{CEC - a_m}{CEC} \qquad (4)$$

where a ratio $(CEC\text{-}a_m)/CEC$ express "unexploited" CEC of MMT; $n_w(MMT)$ was calculated as the water amount released during the dehydration of MMT. By combination of Equations (3) and (4) it holds

$$n_w = n_w(M-MMT) - n_w(MMT)\frac{CEC - a_m}{CEC} \qquad (5)$$

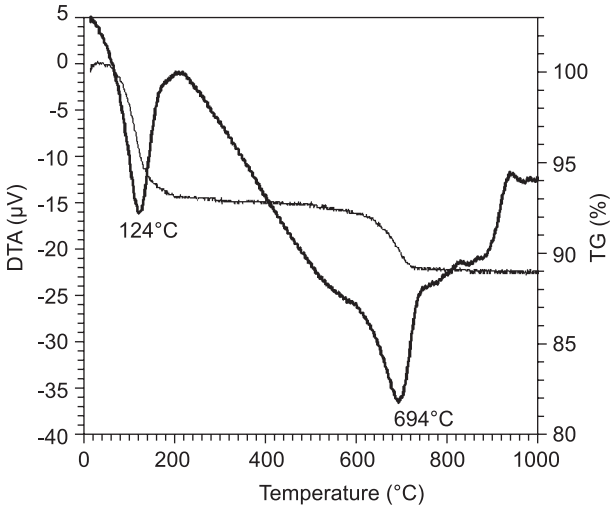

a)

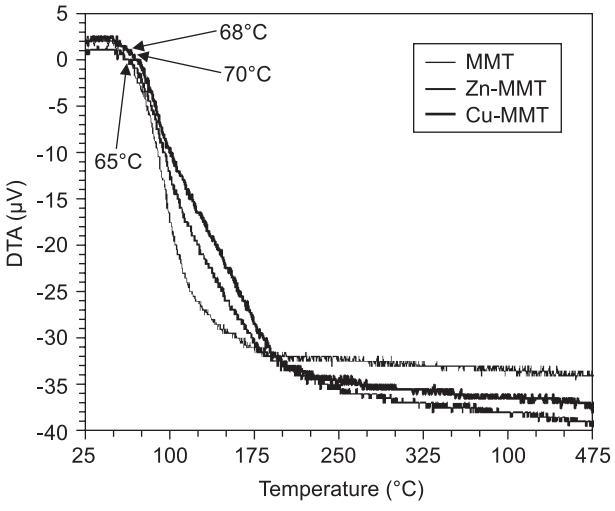

b)

Figure 6. TG/DTA curves of a) MMT at the heating rate of 10 °C/min, b) Zn-MMT and Cu-MMT (5 °C/min).

The initial dehydration temperatures were estimated from the TG curves at sharp decreases of the sample weights at 68°C, 65°C and 70°C for MMT, Zn-MMT and Cu-MMT, respectively. The final dehydration temperatures were estimated as the temperatures when the sample weights were nearly constant, that is at 250°C. The molar ratios water/metal for Zn-MMT and Cu-MMT calculated as $n_w(M)/a_m(M)$ were determined at 6.6:1 and 6.8:1, respectively. These values can be related to the formation of $[Zn(H_2O)_6]^{2+}$ and $[Cu(H_2O)_6]^{2+}$.

CONCLUSION

In this study, the adsorption of Zn^{2+} and Cu^{2+} on natural montmorillonite was investigated. No surface complexes between MMT and these metals were observed by UV-VIS DRS and only their intercalation in the MMT interlayer was confirmed by XRD. Using the DRIFT method, the amounts of interlayer water in Zn-MMT and Cu-MMT were found to be similar. The losses of interlayer water estimated from the TG curves indicated that the intercalated metals were co-ordinated by the water molecules forming $[Zn(H_2O)_6]^{2+}$ and $[Cu(H_2O)_6]^{2+}$.

In order to enhance the adsorbed amounts of Zn^{2+} and Cu^{2+}, MMT was intercalated by EDA prior to the adsorption experiments. The adsorbed amount of Cu^{2+} increased about 28 % (still below CEC) but the amount of Zn^{2+} were about 3-4 fold higher than CEC. In all cases, the Langmuir-Freundlich isotherm fits the adsorption data best, which indicates the metal monolayer formation on MMT as well as on EDA-MMT.

The infrared spectra obtained by the KBr method revealed the formation of $[Cu(EDA)_2]^{2+}$ in the MMT interlayer. The huge uptake of the adsorbed zinc ions on EDA-MMT was explained by extension of the MMT interlayer space by the intercalation of EDA, which enables the following intercalation of the zinc and nitrate ions.

The obtained results imply that montmorillonite can be used as an efficient material for the retention of zinc and copper. The next research will be concentrated on the adsorption of these metals on MMT in real surface and waste waters.

Acknowledgement

The authors would like to thank Dr. T. Grygar (Institute of Inorganic Chemistry of the ASCR, Czech Republic) for the measurements of DR spectra; Dr. Ritz, Dr. M. Valášková and Dr. P. Kozelský (all from VŠB-Technical University of Ostrava) for the measurements of infrared spectra, XRD patterns and TG/DTA curves, respectively. This work was supported by the Ministry of Education, Youth and Sport of the Czech Republic (MSM 6198910016) and by the Regional Materials Science and Technology Centre (CZ.1.05/2.1.00/01.0040).

References

1. Stevens J. J., Anderson S. J.: Clays Clay Miner. *44*, 132 (1996).
2. Kurkova M., Praus P., Klika Z.: Chem. Listy *94*, 241 (2000).
3. Srinivasan K. R., Fogler H. S.: Clays Clay Miner. *38*, 277 (1990).
4. Weiss Z., Klika Z., Čapková P., Janeba D., Kozubová S.: Phys. Chem. Miner. *25*, 534 (1998).
5. Jiang J.-Q., Cooper C., Ouki S.: Chemosphere *47*, 711 (2002).
6. Lim T. T., Tay J. H., Teh C. I.: Water Environ Res. *74*, 346 (2002).
7. Bradl H. B.: J. Colloid Inter. Sci. 277, 1 (2004).
8. Wagner J. F .: Schriftenr. Angew. Geol. Karlsruhe *22*, 1 (1992).
9. Bradbury M. H., Baeyens B.: J. Cont. Hydro. *27*, 223 (1997).
10. Kraepiel M. L., Keller K., Morel F. M. M.: J. Colloid Inter. Sci. *210*, 43 (1999).
11. Strawn D. G., Palmer N. E., Furnare L. J., Goodell C., Amonette J. E., Kukkdapu R. K.: Clays Clay Miner. *52*, 324 (2004).
12. Ikhsan J., Wells J. D., Johnson B. B., Angove M. J.: Colloid. Surf. A. *252*, 33 (2005).
13. Farrah H., Pickering W.F.: Chem. Geol. *25*, 317 (1979).
14. Németh T., Mohai I., Tóth M.: Acta Miner. Petrograph. *46*, 29 (2005).
15. Crus-Guzmán M., Celis R., Hermocím M. C., Koskinen W. C., Nater A. E., Cornejo J.: Soil Sci. Soc. Am. J. *70*, 215 (2006).
16. Guerra D. L., Airoldy C., Viana R. R.: Inorg. Chem. Commun. *11*, 20 (2008).
17. Madejová J., Arvaiová B., Komadel P., Spectrochim. Acta A. *55*, 2467 (1999).
18. Varian Handbook: *Analytical methods for flame spectrometry*, Varian Techtron Pty. Ltd., Springvale 1979.
19. Czechoslovakia state standard; ČSN 720101: *Basic analysis of silicates*. Decomposition, Prague 1974.
20. Sips R.: J. Chem. Phys. *18*, 1024 (1950).
21. Sharma S.; Agarwal G. P.: Anal. Biochem. *288*, 126 (2001).
22. Trojáčková S.: Diploma thesis. VŠB-TU Ostrava, Ostrava 2008.
23. Ding Z., Frost R. L.: J. Colloid Inter. Sci. *269*, 296 (2004).
24. Stadler M., Schindler P.W.: Clays Clay Miner. *42*, 680 (1994)
25. Bergaya F., Vayer M.: Appl. Clay Sci. *12*, 275 (1997).
26. Kevan L.: Pure Appl. Chem. *64*, 781 (1992).
27. Morton J. D., Semrau J. D., Hayes K. F.: Geochim. Cosmochim. Acta *65*, 2709 (2001).
28. Hyun S. P., Cho Y. H., Kim S. J., Hahn P. S.: J. Colloid Interface. Sci. *222*, 254 (2000).
29. He H. P., Guo J. G., Xie X. D., Peng J. L.: Environ. Int. *26*, 347 (2001).
30. Janeba D., Čapková P., Schenk H.: Clay Miner. *33*, 197 (1998).
31. Greenwood N. N., Earnshaw A.: *Chemistry of Elements*, Pergamon Press Plc, Oxford 1984.
32. Kloproge J. T., Mahmutagic E., Frost R. L., J. Colloid Interface Sci. *296*, 640 (2006).
33. Fajnor V., Š., Jesenák K.: J. Therm. Anal. *46*, 489 (1996).